Original Article

Structural Health Monitoring

Structural Health Monitoring
1–17

DOI: 10.1177/1475921718804466
journals.sagepub.com/home/shm
SAGE

Strain and crack analysis within concrete members using distributed fibre optic sensors

Rafał Sieńko[1], Mariusz Zych[1], Łukasz Bednarski[2] and Tomasz Howiacki[1]

Abstract

This article presents laboratory tests, with the purpose being to verify the suitability of standard optical fibres in a tight jacket for advanced strain analysis within concrete members. An optical reflectometer was used to enable the optical signal to be processed on the basis of the Rayleigh scattering phenomenon, so that strains and/or temperature changes were determined along the length of the measuring fibre. The measurements were carried out continuously in a geometrical sense (distributed measurements), with a spatial resolution starting from as fine as 5 mm. The arrangement of optical fibres inside the heterogeneous concrete medium and on its surface allowed for the identification and detailed analysis of local phenomena such as cracks. Remote and early location of structural damage with an estimation of its scale provides new opportunities for the monitoring of the structural health of reinforced concrete structures, facilitating the interpretation of its behaviour as well as failure risk management based on comprehensive and reliable measurement data. If traditional spot techniques are used, this approach is not possible. The aim of the initial studies was to analyse the strain distributions over compressed and tensioned measurement sections located on the surface of a cylindrical specimen of concrete. In the tests which followed, the reinforced concrete rod was eccentrically tensioned with fibre optics installed inside. Qualitative and quantitative verification of crack widths was made, with a narrow range up to 0.05 mm and a wider one to 0.30 mm. The results of the studies show very good accuracy of optical fibre sensor technology as a reference technique during the analysis of microcracks and narrow cracks, and moderate accuracy in the case of wider cracks. Despite using optical fibres in a tight jacket which mediates in strain transfer, the results obtained can be very suitable for the assessment of the structural condition of the member under consideration. It is also worth noting that the tests conducted indicate the effectiveness of distributed optical fibre technology for the analysis of concrete homogeneity and its structural behaviour within compressed areas, as it is possible to calculate strains over measuring bases that start from lengths as short as 5 mm.

Keywords

Distributed fibre optic sensors, strain measurements, cracks in concrete, Rayleigh scattering

Introduction

Investigations of concrete structures are performed using sensors which operate on the basis of different physical phenomena. Mechanical, electrical resistance, inductive and vibrating wire sensors[1] are commonly used. Their common denominator is the ability to carry out measurements of a given physical quantity at a local scale, that is, over the length of a measuring base (Figure 1(a)). Distribution of the measured quantity along a given line can only be analysed by installing several sensors within this line (quasi-continuous measurements –Figure 1(b)). This approach, however, involves the necessity of incurring significant financial costs, which is why it is only occasionally used. Optical fibre technology introduces new possibilities, especially with regard to the quality and number of items of information to be obtained, but also in the economic context. It is based on light scattering and allows for strain

[1]Faculty of Civil Engineering, Krakow University of Technology, Kraków, Poland
[2]AGH University of Science and Technology, Kraków, Poland

Corresponding author:
Mariusz Zych, Faculty of Civil Engineering, Krakow University of Technology, Warszawska 24, 31-155 Kraków, Poland.
Email: mzych@pk.edu.pl

and/or temperature measurements to be made with a spatial resolution of 5 mm along the length of the optical fibre[2,3] (distributed fibre optic sensors (DFOS)). From an engineering point of view, such measurements can be considered as continuous measurements in a geometric sense (Figure 1(c)).

A number of studies in the area of distributed optical fibre measurement technology have been conducted under laboratory conditions over the last few years. Attention was paid to embedding fibres into a concrete medium,[4] detecting damage (cracks) within concrete structures,[5] and analysing their strain and temperature distributions[6] using different optical phenomena such us Brillouin[7] or Rayleigh[8] scattering.

This led to pilot applications within the structural monitoring of real engineering structures. A wide range of practical applications, including a historical perspective, have been presented in previous studies.[9,10] There are some examples of optical fibre measurements carried out on bridges, for example, a concrete road bridge (Naples, Italy) with a steel road bearing structure[11] or a concrete bridge[12] opened in 1969 (Potenza, Italy) with a span of 70 m and very untypical geometry. The authors of the previous papers[13–15] paid their attention to applying optical sensors to a varied range of engineering structures, including bridges, dams, geotechnical structures, pipelines, historical buildings and other structures such as a concrete cooling tower. Other practical examples, as well as methods and tools, relating to the use of optical fibre sensor technology for structural health monitoring have been widely described in a number of studies.[16,17]

Despite much research and in situ applications, there are still a number of technical problems, primarily regarding adhesion between the measuring fibre and the surrounding medium,[18,19] which allows a reliable transfer of the strains from the member under test to the fibre glass core. In addition, the researchers are working on the creation of computational algorithms and advanced numerical models,[4] taking into account nonlinear relations between solid elements representing the individual layers mediating in strain transfer. Some mechanical properties of fibres and their modelling over their lifetime in different conditions have been presented.[20] There are also some difficulties with the installation of slender optical fibres into the analysed medium (e.g. concrete), because of the possibility of breaking the fibre or occurrence deviations from the designed position. Still, the important challenge is to analyse the cracks in the member based on the strain distribution along the length of the fibre. Such attempts, including advanced mathematical models, have already been described in the literature,[21,22] but there are still no clear guidelines on how to mount and choose the type of measuring fibres and to apply

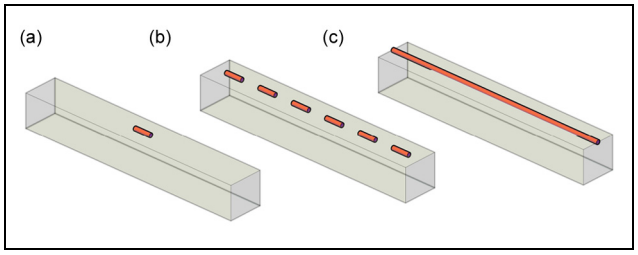

Figure 1. Measurement scheme: (a) spot, (b) quasi-continuous and (c) distributed (geometrically continuous).

algorithms to process the raw measurement data into engineering values that are useful and intuitive to interpret.

These guidelines should include, among others, the following:

- Sensor limit strains, enabling the measurement of cracks with expected width in a given structural member;
- Adhesion parameters between the fibre coating and the concrete as well as the glass fibre;
- Elasticity of the protective coating and its impact on the results of crack width measurements;
- Selection of a calculation model for transferring strains from the medium under test through protective coatings on a glass measuring fibre.

In the following chapters of this article, the results of studies carried out in this field in the Laboratory of the Institute of Building Materials and Structures (Faculty of Civil Engineering, Cracow University of Technology, Poland) are presented, also indicating further directions for research. The main aim of these studies was to verify the suitability of standard optical fibres with a tight jacket for advanced strain and crack analysis within concrete members under test. Optical measuring device based on the Rayleigh scattering phenomenon was used, so that strain distributions along the entire length of the fibre were determined with a spatial resolution starting from 5 mm.

Principles of operation and construction of DFOS

Nowadays, the fibre most commonly used for distributed optical fibre measurements is a glass one in which an electromagnetic wave is transmitted along a 9-μm-diameter core. This is rendered possible due to the phenomenon of total internal reflection which occurs on the contact surface between the core and the surrounding glass cladding which has a slightly different

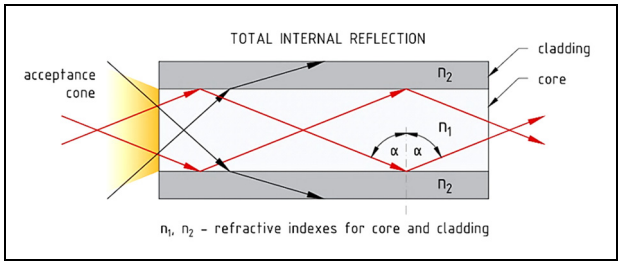

Figure 2. The principle of total internal reflection within the optical fibre (in order to provide proper readability of the figure, the diameter of the core and cladding are not scaled proportionally).

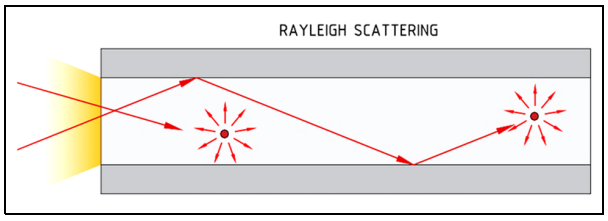

Figure 3. The Rayleigh scattering scheme within the fibre core.

refractive index. Figure 2 shows this phenomenon schematically.

In telecommunication applications, the fibre should be as pure as possible, that is, free from microcracks, micro-impurities, imperfections or local changes in density, which cause light wave energy losses over the length of the optical fibre.[23] One of the reasons is the Rayleigh scattering phenomenon[24] occurring in every fibre cross section (see Figure 3) as a result of the particle structure of matter causing a heterogeneity of refractive index at microscale. This is accompanied by the backscattering phenomenon. The light reflected from the imperfection of the glass structure moves backward relative to the original direction of motion. Scattering amplitude is a random but constant property for a given fibre.

Because of the changes in fibre length caused by mechanical or thermal strain, the distance between local imperfections will also be changed. This will be seen as a shift in the backscatter wave frequency spectrum. The actual scattering profile for mechanically or thermally loaded fibre is compared with a reference profile with a spatial resolution starting from 5 mm. In measurements of engineering structures, this resolution provides a new quality to the interpretation of the results. The spectrum shift $\Delta\upsilon$ is proportional to the linear combination of strain changes $\Delta\varepsilon$ and the temperature changes ΔT according to the following formula[25]

$$\frac{-\Delta\upsilon}{\upsilon} = K_T\Delta T + K_\varepsilon\Delta\varepsilon \tag{1}$$

where υ is the mean optical frequency (Hz), K_T is the temperature calibration constant ($^\circ C^{-1}$), K_ε is the strain calibration constant, ΔT is the temperature change (°C) and $\Delta\varepsilon$ is the strain change ($\mu\varepsilon$).

In the case of the total elimination of temperature-induced strains, which is only possible in laboratory conditions, the change in strains caused by mechanical loads is given by[25]

$$\Delta\varepsilon = \frac{-\lambda_{cen}}{cK_\varepsilon}\cdot\Delta\upsilon \tag{2}$$

where λ_{cen} is the centre scan wavelength (nm) and c is the speed of light (m/s).

During the research presented in the following sections of this article, the results were not compensated for thermal influences, as stable external conditions have been ensured. An OBR 4600[25] optical backscatter reflectometer manufactured by Luna Innovations (Figure 4(a)), based on Rayleigh scattering, was used to measure the distribution of strains along the length of the fibre. The selected technical parameters of the reflectometer are summarised in Table 1.

When performing distributed measurements, it is worth initially assessing to what level of strain adhesion is maintained between the measuring element and the medium under test, allowing for appropriate strain transfer. This adhesion depends largely on the construction of the fibre used. The measuring element is only a glass core (9 μm diameter) coupled with a glass cladding (125 μm in diameter). During the production process, the cladding is coated with lacquer layers, which makes it possible to use the brittle fibre in practical applications. The construction of the subsequent layers, which are mainly dedicated to ensuring that the optical fibres are protected from accidental mechanical damage, can vary greatly depending on the application. All layers will mediate in the transfer of strain from the medium being examined to the glass core. In the case of very high strain values, for example, in the immediate area of the cracks in the concrete member, there is a risk of loss of adhesion on the concrete–fibre contact surface and/or between the particular layers within the fibre. This will cause difficulties in interpreting the measurement data within these areas (smoothing the graph). Therefore, knowledge about fibre construction and the mechanical parameters of all the layers used for its construction is very important in the context of assessing the usefulness of a particular fibre for distributed strain measurements. A cross section through a standard fibre is shown in Figure 4(b).

For fibre optic technology to be widely used in civil engineering applications, the proposed solutions should be optimised not only for the quality of the information obtained, but also for economic reasons. Hence, the

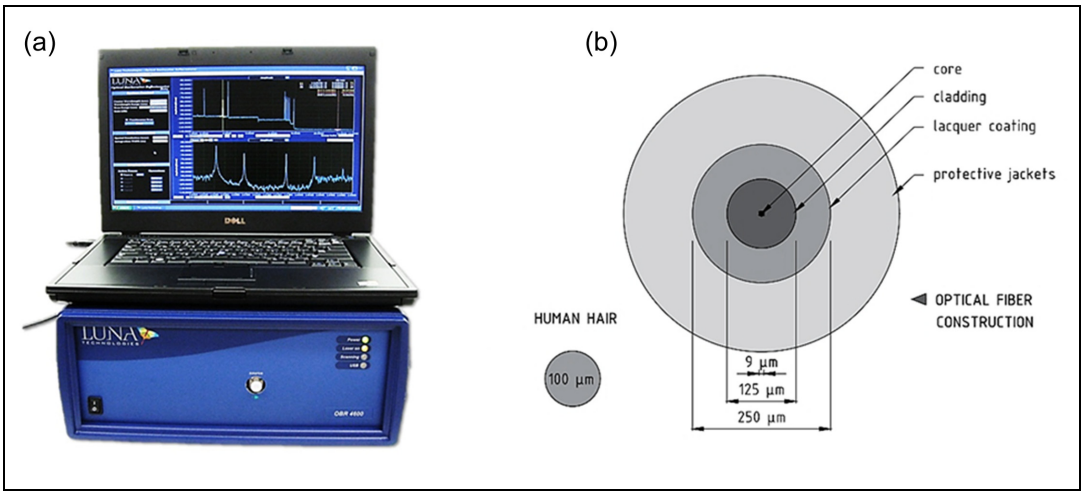

Figure 4. (a) Optical reflector OBR 4600 manufactured by Luna Technologies and (b) cross-section through standard single-mode optical fibre.

Table 1. Selected technical characteristics of the OBR 4600 reflectometer.

Parameter	Value	Unit
Maximum measuring length		
Standard mode	30 or 70	m
Extended mode	2000	m
Distributed measurements		
Spatial resolution	±5	mm
Temperature resolution	±0.1	°C
Deformation resolution	±1.0	με

standardised single-mode telecommunication optical fibre SM 9/125 in a tight jacket (outer diameter of 0.9 mm), which is widely used in the telecommunications field, was used during the tests. The aims of this research included, among other things, verifying the usefulness of such fibres for advanced strain and crack analysis within members made of concrete.

Concrete cylinder in an axial compression test

Purpose of the study

The aim of the study was to investigate the possibility of using fibre optic technology for simultaneous measurements of strains caused by compression (to assess the structural homogeneity of the concrete) and strains caused by tension (allowing for the identification of cracks perpendicular to the measuring line). The objective was to determine whether the proposed method of mounting optical fibre on the surface of existing structures made of concrete could be effective in the context of the correct assessment of their technical condition.

Specimen preparation

The specimen was made from C40/50 class concrete as a standard cylinder of 300 mm height and 150 mm base diameter, as commonly used in tests on the properties of concrete. The optical fibre was installed on the cleaned and degreased surface of the specimen by gluing it with a two-component epoxy adhesive, so that a total of five measuring sections (A–E) were formed (Figure 5(a)). Three longitudinal sections (A–C) of 130 mm length were uniformly distributed 120° apart in the compression direction. Two circumferential sections (D–F), equal to $\pi\text{Ø} = 470$ mm, were installed at a spacing equal to the length of the longitudinal section and were located in the direction of the parallel tensile stresses. The visualisation of the measuring line on the peripheral surface of the cylinder, including five sections, is shown in Figure 5(b).

The lower and upper surfaces of the specimen were aligned by grinding, providing a uniform load transfer from the blocks of the materials testing machine and avoiding the formation of local concentrations of stress that could lead to the untimely destruction of the specimen.

Conduct of the study

The research was conducted in two stages. In the first stage, the specimen was gradually loaded (0.1 MPa/s) to an average compressive stress of 40 MPa and then relieved to 2 MPa. In order to verify the measurement results, a reference technique was used by means of three external extensometers along the specimen with a measurement base of 170 mm. The sampling frequency of the external extensometers was 0.1 Hz, while the

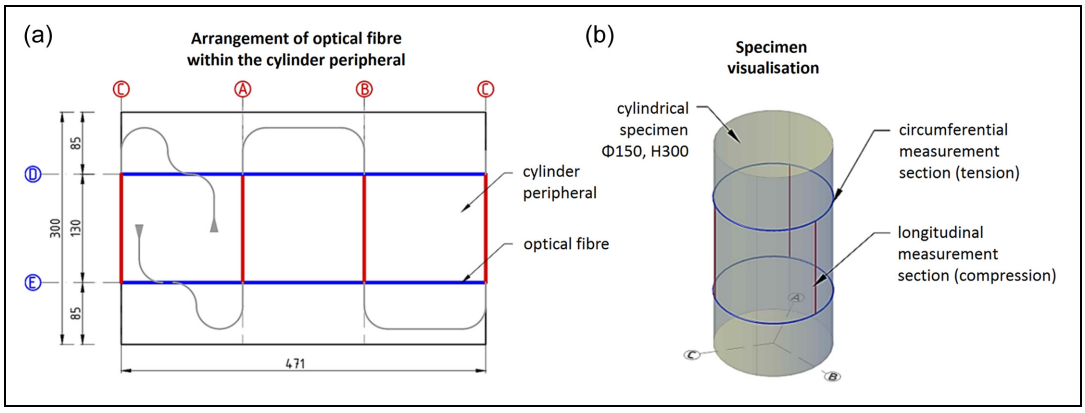

Figure 5. (a) The arrangement of optical fibre on the peripheral surface of the cylinder and (b) visualisation of the concrete specimen examined.

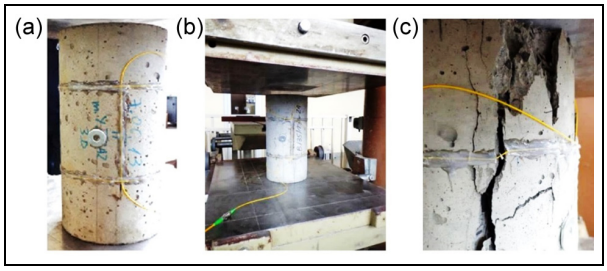

Figure 6. (a) View of concrete specimen prepared for tests, (b) view of the measurement stand just before the start of the test and (c) close-up of a specimen after destruction.

optical fibre was recorded every few seconds. In the second stage, the specimen was subjected to compression until it was destroyed, after having previously removed the reference extensometers. Figure 6 shows the view of specimen with measuring fibres before the tests (Figure 6(a)), a view of the measurement stand (Figure 6(b)) and the specimen close-up after its destruction (Figure 6(c)). The length of the optical sensor measurement bases spaced along the length of the fibre was set during post-processing to 5 mm (within these bases strains were averaged) and the distance between the successive sensor centres was also set to 5 mm.

Results and conclusion

The distributions of strain along the length of the entire measuring line during the second stage of the tests, that is, under increasing load until destruction of the specimen, are shown in Figure 7. The results from the first stage (loading up to 40 MPa and releasing to 2 MPa) are analogous to the second, but without a so clearly visible development of local extremes of strain corresponding to the occurrence of cracks perpendicular to the specimen circumference. Tensile strains are indicated with a '+' sign, while compression strains are indicated with a '–' sign.

In the case of sections located along the height of the specimen, where compressive stress occurred, the shape of the strain distribution is more uniform (smaller differences between local extremes) than in the case of peripheral sections where tensile stress as well as microcracks occurred. Mathematical verification was performed by determining the average coefficient of variation for strain distributions along the particular measurement sections, which expresses the variance of strain with respect to the arithmetic mean

$$V = \frac{s_\varepsilon}{\varepsilon_m} = \frac{n\sqrt{\dfrac{\sum_{i=1}^{n}(\varepsilon_i - \varepsilon_m)^2}{n-1}}}{\sum_{i=1}^{n}\varepsilon_i} \tag{3}$$

where V is the coefficient of variation for strain distribution, s_ε is the standard deviation, ε_m is the mean strain along the section considered, ε_i represent the values of successive strains measured along the section considered and n is the number of sensors along the section considered.

For the first stage of the study, the mean value of the coefficient of variation for the distribution of longitudinal strains was 30.9%, while for peripheral strains it was 30.3% (moderate variation). These values are close to each other due to the fact that in the first stage compressive stress was limited to 40 MPa, making it impossible for crack widths to develop significantly in the meridian direction. In the first stage of the study, good compatibility was obtained between the longitudinal optical fibre measurements and the reference technique – see Figure 8.

The first microcracks formed along the circumference during the concrete hardening process in addition

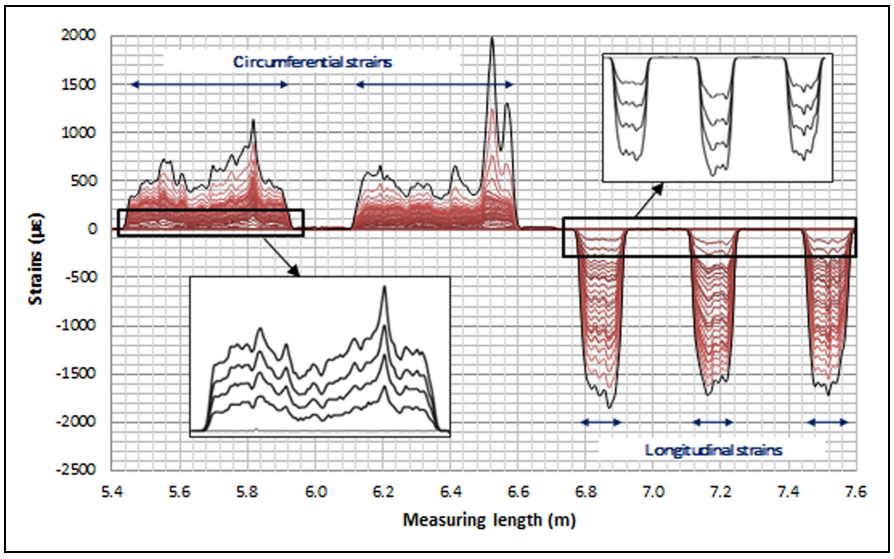

Figure 7. Strain distributions along the entire length of the fibre in the second stage of the tests (the last plot corresponds to the moment just before the specimen was destroyed).

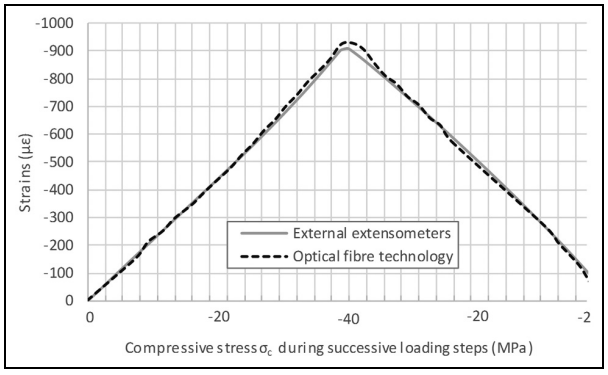

Figure 8. Comparison between the results obtained from external extensometers and optical fibre measurements averaged over the same measurement base (first stage of research).

to those forming in the first stage of the studies. When increasing the load in the second stage, the differences between the respective crack widths decreased gradually.

In the second stage, the external extensometers were removed to protect them from damage. The results obtained correspond in a qualitative manner to the results from the first stage, but a significant development of the local tensile strain extreme values was observed, which is related to a large increase in the meridian crack widths during the final load steps. After the stress exceeded 40 MPa, the largest widths were only measured in a few cracks, which were those that in the end were responsible for the destruction of the specimen. In the last measurement made just before the specimen was destroyed, the coefficient of variation for strain distributions caused by tension was equal to 60.0% – see Figure 9. The coefficients of variation for the strains caused by compression were lower than those in the first stage, which is related to the sealing of the concrete microstructure.

The coefficient of variation of the measured strain distribution can be interpreted as a qualitative measure of crack development within the concrete surface. Thus, in the case of strains causing compression (along the longitudinal direction), the value of this coefficient was almost constant during the entire test (cracks did not significantly arise opposite to the peripheral sections). As a result, there is no direct relationship between V by the longitudinal strain and V by the peripheral strain.

The calculated variation coefficient takes into account also the measuring error of the sensor; however, compared to the measured strain values ($\approx$2000 $\mu\Delta$), this error (± 1 $\mu\varepsilon$) is negligibly small.

It should be noted that in the case of a theoretical analysis, assuming homogeneity of the concrete and its operation within the linear-elastic range, the strain distribution along the individual sections being measured should be a constant function (variation coefficient equal to 0%). This information is provided by external extensometers which provide average values from a given measuring base. The use of optical fibres allows a much more comprehensive evaluation to be made of the structural behaviour of the member under test.

It should also be pointed out that the strain distribution within the sections used for measurement retains its shape from the beginning of the test through all the subsequent load steps. It is therefore possible to identify

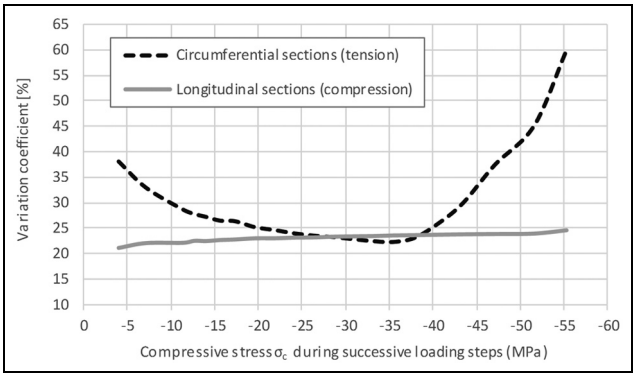

Figure 9. Mean coefficient of variation (%) for strain distributions calculated for longitudinal and circumferential sections in successive load steps during the second stage of research.

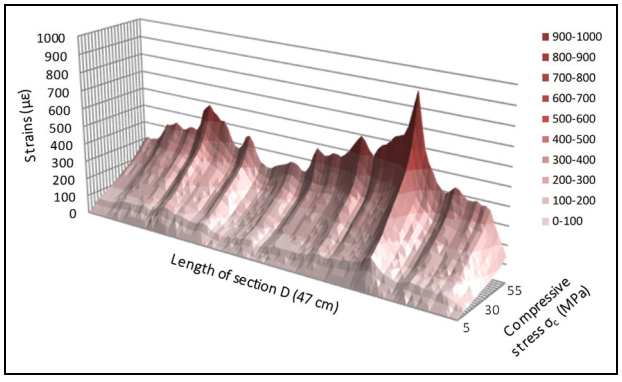

Figure 10. Example of a spatial graph of longitudinal strain distributions for section A caused by compression in the length and compressive load σ_c fields.

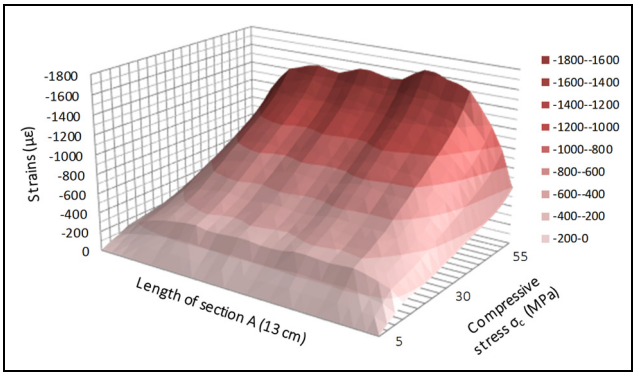

Figure 11. Example of a spatial graph of circumferential strain distributions for section D caused by tension in the length and compressive load σ_c fields.

where the concrete structure is the weakest (local strain extremes) at an early stage of loading, that is, even when the concrete is not cracked or when microcracks are invisible to the naked eye and do not yet significantly affect the structural behaviour. This approach provides a real opportunity to improve the safety of engineering structures by identifying and analysing phenomena that are not recordable by conventional measurement techniques. Since the measured strain values are a function of two variables, it will be convenient to present them in spatial graphs, where the stress and length fields are defined on the horizontal axes (Figures 10 and 11).

Testing reinforced concrete bar for eccentric tension

Description of the member under test

The purpose of the tests was to verify the usefulness of standard optical fibres for strain measurement within a reinforced concrete member, operating in a cracked state, by qualitative and quantitative evaluation of the cracks occurring during the load test. The calculated (on the basis of fibre strain records) crack widths were verified by comparison with the standard measurement made by a Brinell magnifying glass. The analysis was carried out in two stages, including narrow (up to 0.05 mm wide) and wider (up to 0.30 mm wide) cracks.

The rod element being tested was made of C20/25 class concrete with the dimensions of 77 × 110 × 1050 mm^3 (Figure 12(a) and (b)). A reinforcement bar of 16 mm diameter was placed inside the concrete medium. This bar was made of ribbed RB-500W steel which has a characteristic yield strength value of 500 MPa. The optical fibre was set inside the element in six different positions (marks from A to F – see Figure 12(b) and (c)).

As shown in Figure 12, fibre optics were placed along the member length in six different positions. For this purpose, the prism-shaped form was prepared. Within its 110 × 77 mm^2 bases, the holes were drilled to pass through the measurement fibres. The initial tension of the optical fibres was provided by anchoring with the epoxy resin in the holes. As a result, the necessity of applying intermediate fibre supports along the length of the specimen, which would disturb the measurements, was eliminated. What is more, to facilitate concrete mix compacting without damaging the optical fibres, the maximum diameter of the gravel aggregate was 8 mm and the concrete with semi-liquid consistency was used. Within the C section, the fibre was glued to the degreased reinforcement bar using the epoxy resin parallel to the longitudinal rib.

In the post-processing of raw data, the length of the optical fibre sensor measurement base was set at 10 mm and the distance between the successive bases was

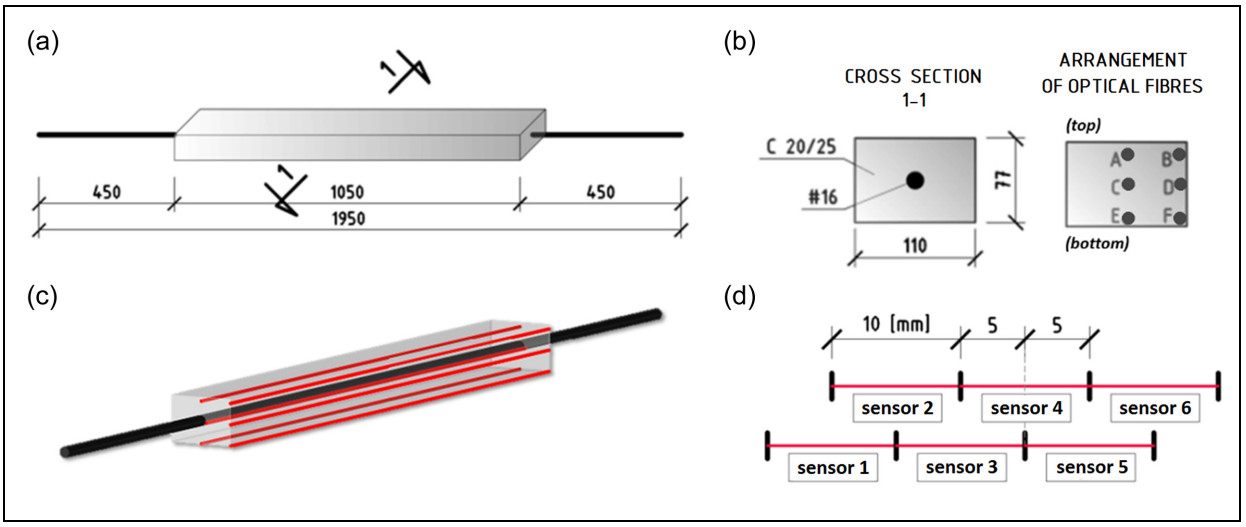

Figure 12. (a) Dimensions of the specimen under test, (b) cross section through the specimen with the locations of optical fibres, (c) visualisation of the member analysed and (d) scheme of arrangement of sensor bases along the length of the fibre.

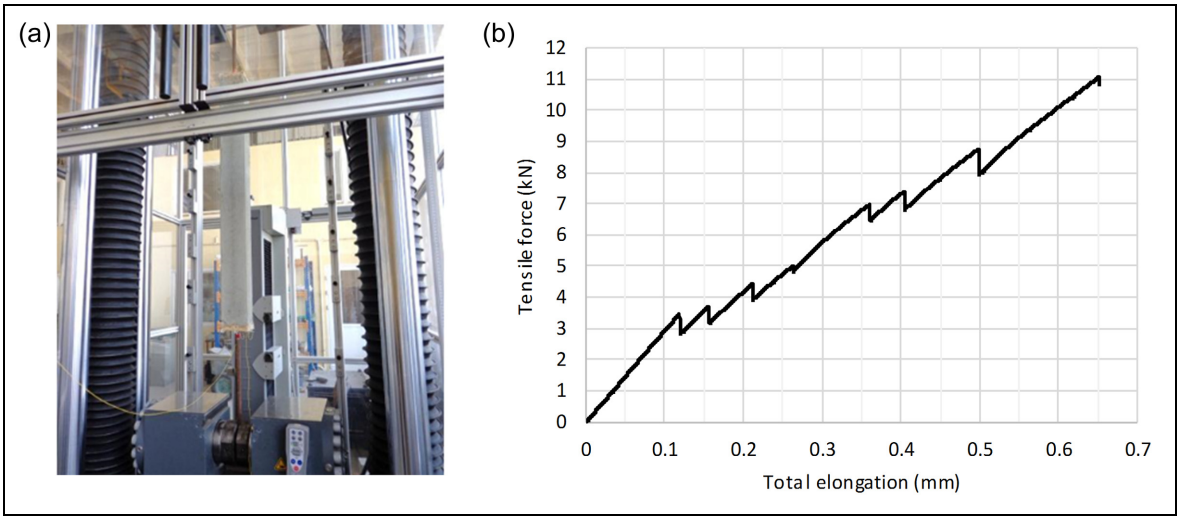

Figure 13. (a) View of the rod under tensile testing and (b) the relationship of total elongation between the jaws of the materials testing machine with the tensile force applied to the member in the first stage of research.

5 mm. This means that the sensor bases overlapped by half of their lengths (Figure 12(d)).

Stage I – study methods and presentation of results

The member was mounted in the Zwick/Roell materials testing machine (Figure 13(a)) and stretched in two stages. In the first stage, tensile force was introduced through the ends of the reinforcement bar with a speed of 0.01 mm/s, reaching the value of 12 kN. Figure 13(b) shows the graph of the total elongation between the jaws of the materials testing machine and the force applied to the member during the first stage of research.

The load was applied eccentrically to the shorter edge of the cross section not only because of the specimen geometry, but also because of the experimental conditions, which makes this phenomenon complex and difficult to evaluate. Thus, more intense drying of the member's upper surface (the other surfaces were covered with the shuttering during the hardening process of the concrete), which caused curving of the specimen, was also taken into consideration. Another source of eccentricity was caused due to the rigid mounting of the bar in the jaws of the materials testing machine.

Figure 14 shows the fibre strains within the individual sections being measured which were recorded before

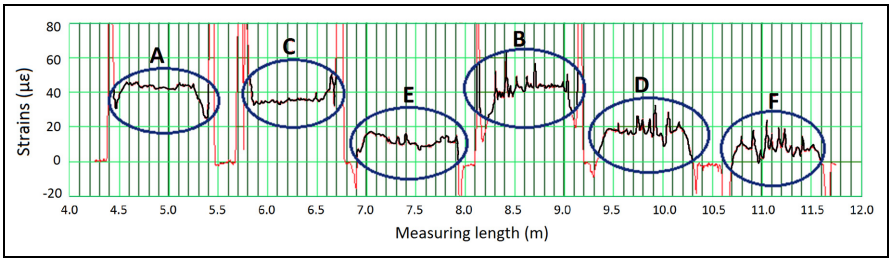

Figure 14. Optical fibre strains recorded within individual measurement sections (A–F: see Figure 12) before the concrete became cracked.

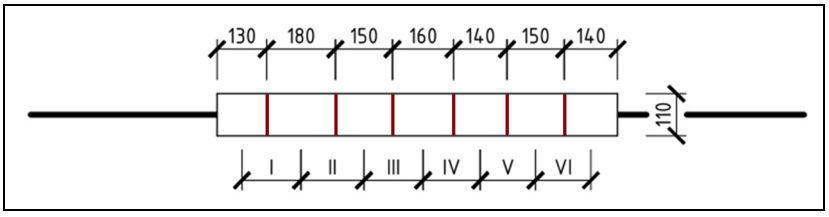

Figure 15. Location of cracks on the surface of a reinforced concrete rod on the more tensile surface of the rod in the first stage of studies with the designation of sections (I–VI) between successive cracks.

the concrete became cracked. Sections A, B and E, F represent the strains at the more and less tensile surfaces, respectively. The average strain on the more tensile (upper) surface is 44 $\mu\varepsilon$ and that on the less tensile (lower) surface is 11 $\mu\varepsilon$. On this basis, the mean load eccentricity $e_{mean} = 7.7$ mm $\approx$ h/10 was determined. It can be seen from Figure 14 that the strain distributions measured along the optical fibres located near the surface of the element (B, D, F) show considerable variation. This is due to the microcracks created by the internal stresses caused by the surface shrinkage phenomenon, which derives from the drying of the concrete matrix. As a standard, the shrinkage is measured on the basis of $0.1 \times 0.1 \times 0.5$ m^3 concrete beams with a 400-mm gauge, so that the measurement is averaged over almost the entire length of the element. In the case of fibre optics, the measurement bases were so short that local changes were recorded in the microcracks.

Figure 13(b) shows the dependence of the total elongation between the jaws of the materials testing machine and the tensile force that was applied to the member. A reduction in the stiffness of the test rod was observed during the successive stages of cracking of concrete. The eccentric load was confirmed through the development of and changes in the crack widths on the lower and upper surfaces of the member. At first, cracks formed on the more tensile (upper) side and, as a result of the progressive redistribution of stresses in the concrete, they developed gradually on the opposite surface. All the critical cracks developed during the application of the load up to a level of 10 kN and these extended further during the second stage of the research (Figure 15).

The changes in strain distributions within the individual fibre sections embedded in concrete and glued to the reinforcement bar, recorded during the first stage, are shown in Figure 16. In Figure 16(a) and (b), strains measured by fibres located closer to the more tensile surface are shown for two load levels, that is, 6 and 10 kN. At a load of 6 kN, there are three characteristic locations of the large strains confirming the appearance of three cracks. At a load of 10 kN, the number of cracks identified by the local strain extremes doubled. The measurements also show that the strains in the areas between the cracks are very small and limited to the limit strains of tensile concrete $\varepsilon_{ctu} \approx 0.08‰$ (80 $\mu\varepsilon$) (for 8-day concrete). From the graphs presented, it can be concluded (in accordance with the theory of reinforced concrete structures) that the strain of the fibre is greatest within the cross section through the crack and decreases with distance from the crack. However, due to the loss of adhesion between the fibre core and the concrete in the vicinity of the cracks, these strains cannot be identified exactly as a deformation of concrete. This phenomenon is confirmed in Figure 16(b) for cracks 1 and 2, where the extreme strain values occur at the load level of 6 kN.

However, in the next loading step (10 kN), these strains are smaller, but cover a wider area in the immediate vicinity of the cracks. This phenomenon is related to slip at the surface where contact is maintained between the fibre jacket and the concrete, as well as

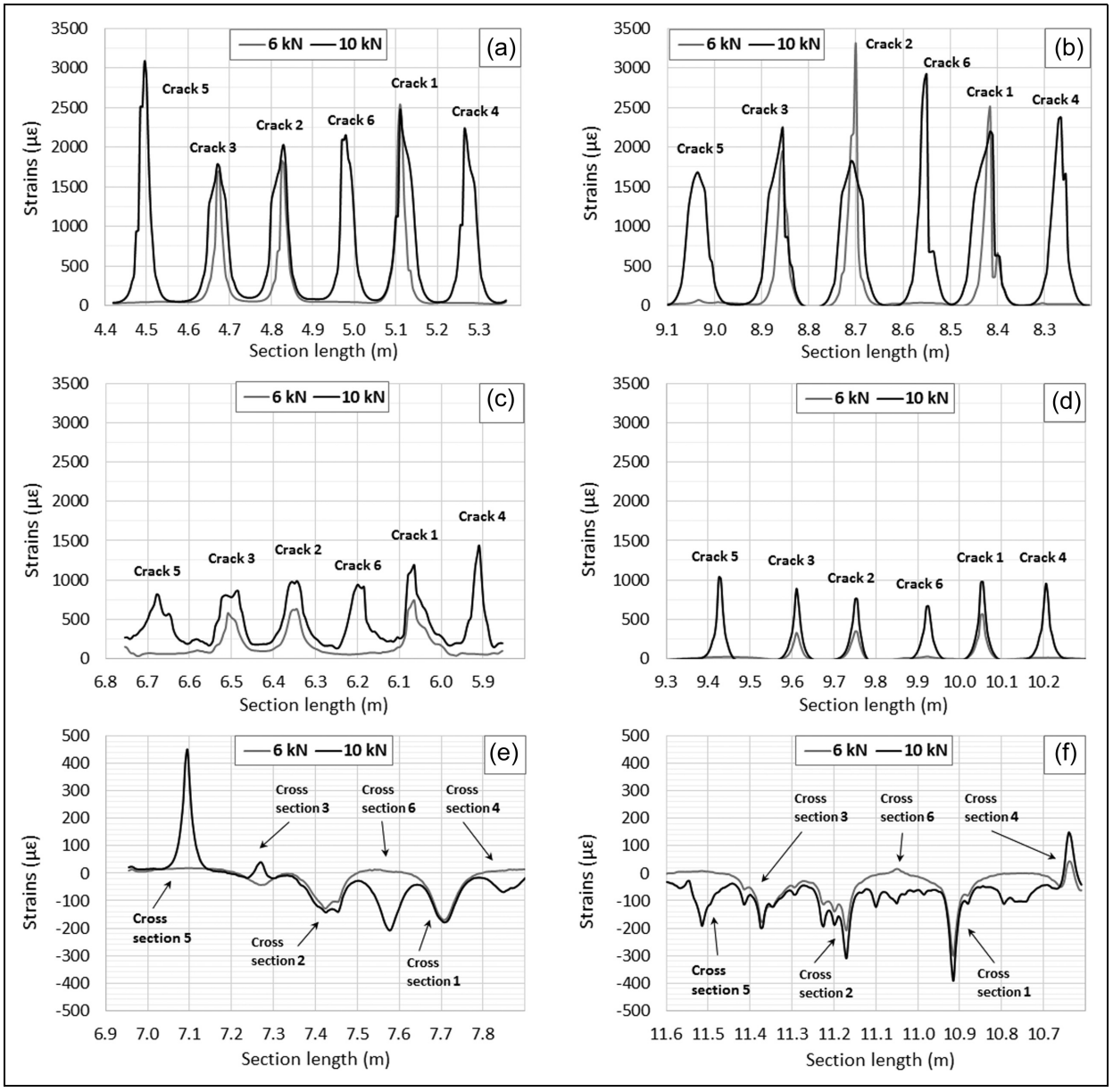

Figure 16. Changes in optical fibre strains measured during the first stage of research on successive measurement sections (Figure 12(b)): (a) top centre, (b) top right, (c) on the reinforcing bar, (d) centre right, (e) bottom centre and (f) bottom right.

between the jacket and the optical glass core with lacquer coating, placed inside the jacket. Finite element analyses of this phenomenon are currently being conducted in Poland by a range of specialists in the field of structural mechanics and photonics together with the authors of this article. Coatings with various mechanical properties (Young's modulus, friction coefficient) and various adhesive agents are tested. The main aim of this research is to find the optimal coating that will allow utilising the full measurement range of the fibre itself. Simultaneously, it must be mathematically possible to describe the mechanism of transferring the strain from the medium under test to the measuring fibre.

Figure 16(c) shows the changes in strain of the fibres glued to the steel bar, which were the basis for determining the stress (Figure 17). For the calculations, the steel's elastic modulus was assumed to be E_s = 200 GPa. The highest strains are observed in cross-sections through the cracks and the smallest between the cracks, where concrete also has its contribution in withstanding the tensile force. The actual stress in the bar within the crack cross-section is not as great as would appear from the graph in Figure 17. The reason for this is that the strains from the steel rod are not actually transferred to the fibre (glass core). The obstacle is the protective fibre jacket and its

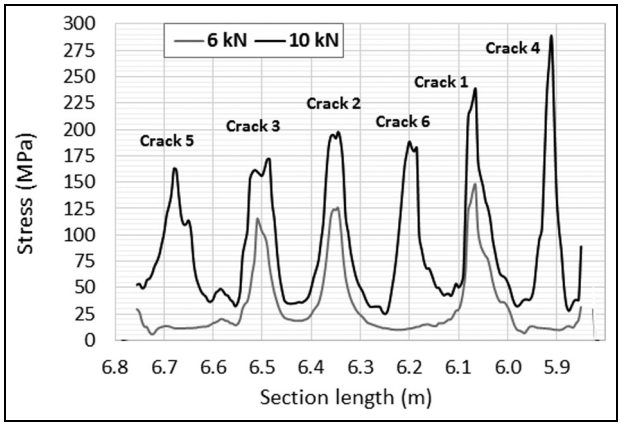

Figure 17. Stress changes in a reinforcing bar calculated on the basis of strains measured by the glued section of optical fibre C (first stage of research).

adhesion to the concrete. The strains within the crack cross-sections measured by the fibre optics C (on the rod) and D (on the lateral surface of the cross-section) are of the same order. This means that the impact of the cracks was dominant in the strain measurements on the bar. The analysis of this issue is certainly worth taking into account in future research.

Figure 16(d) shows the changes of fibre strain in the middle of the member. Due to the eccentric tensioning of the bar, these strains are less than half the value of the strains recorded on the more tensile edge (Figure 16(a)). Figure 16(e) and (f) shows strains on a less tensile surface. These strains are positive or negative, depending on the degree of crack development along the shorter edge of the cross section.

On the basis of the strains measured (Figure 16), the fibre elongations were determined on the given measurement bases with a length of 10 mm (Figure 18). Table 2 summarises the total elongations of the optical fibre within the sections I–VI defined between the cracks (Figure 15). The elongations calculated this way can be equated to the upper limit of the crack opening width. These values should be reduced by the elastic deformations of concrete occurring between the cracks.

In Table 2, the width of a crack occurring on the lateral surface (section B) measured by a Brinell magnifying glass is also presented. At a load of 10 kN, a uniform cracking was recorded within the upper surface of the member with crack widths measuring from 0.038 to 0.054 mm. Taking into account the accuracy of the Brinell magnifying glass reading (±0.0125 mm) and the fact that the reference measurement was performed in a different plane to the optical fibre measurements, the compatibility of both methods is very good and the optical fibre measurement should be considered as more precise. The average differences in the measurements between the Brinell glass and optical fibre (Table 2) for the tensile loads of 6 and 10 kN are, respectively, 0.029 mm – 0.025 mm = 0.004 mm (difference 16%) and 0.050 mm – 0.045 mm = 0.005 mm (difference 10%). Thus, the usefulness of the fibre optic technology for recording very narrow crack widths of about 0.01 mm has been confirmed. This conclusion has a significant practical importance, because it relates to those cracks that are difficult to identify without a Brinell magnifying glass. In addition, research has confirmed the usefulness of distributed optical fibre strain measurement technology for the analysis of wider crack widths of 0.05 mm, which are visible to the naked eye.

Stage II – study and presentation of results

The aim of the second stage of the research was to evaluate the quality of the optical fibre strain measurements during significantly greater loads and thus much wider

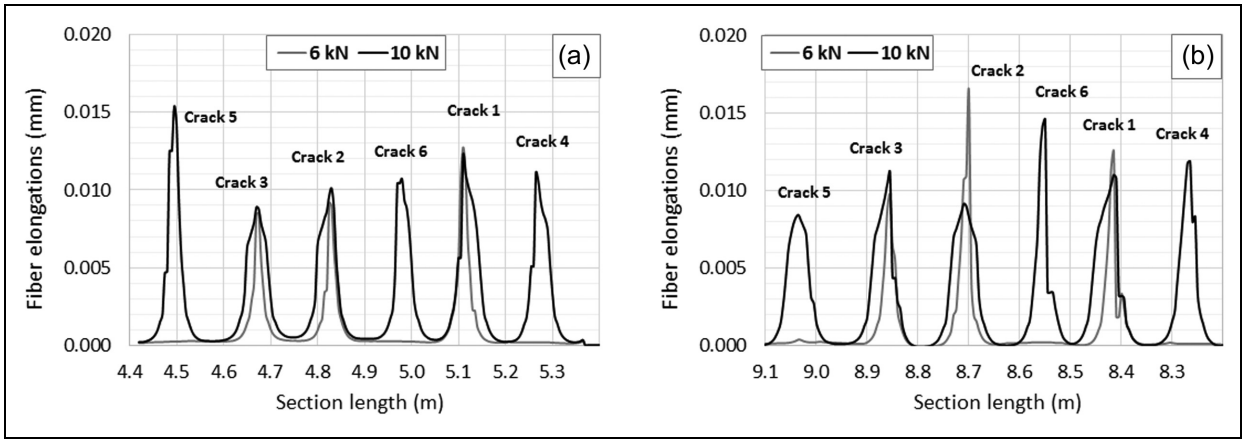

Figure 18. Changes in elongations of selected optical fibres within the sections defined in Figure 15: (a) top centre and (b) top right.

Table 2. Total elongations of the fibre within the sections defined in Figure 15 (I–VI) in the first stage of research (mm).

Section	(kN)	Elongations (mm) on sections corresponding to individual cracks						Mean value (mm)
		I	II	III	IV	V	VI	
A	6/10	0.004	0.025	0.026	0.004	0.035	0.004	0.029/0.048
		0.049	0.048	0.048	0.044	0.052	0.046	
B	6/10	0.003	0.025	0.033	0.002	0.029	0.002	0.029/0.045
		0.043	0.046	0.049	0.038	0.054	0.041	
B	6/10	–	0.025	0.025	–	0.025	–	0.025/0.050
Brinell magnifying glass		0.05	0.05	0.05	0.05	0.05	0.05	
C	6/10	0.004	0.021	0.005	0.019	0.017	0.007	0.019/0.033
		0.028	0.035	0.032	0.035	0.034	0.036	
D	6/10	0.000	0.006	0.000	0.003	0.003	0.001	0.004/0.009
		0.011	0.011	0.007	0.007	0.009	0.011	
E	6/10	0.002	–0.001	–0.005	0.000	–0.006	0.001	–0.001/–0.002
		0.008	0.000	–0.006	–0.007	–0.007	–0.002	
F	6/10	0.000	–0.006	–0.006	0.000	–0.006	–0.001	–0.003/–0.007
		–0.006	–0.008	–0.009	–0.006	–0.011	–0.001	

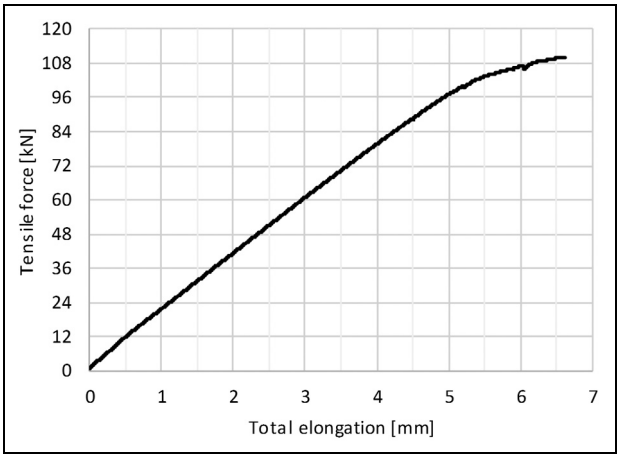

Figure 19. Dependence of total elongation between the jaws of the materials testing machine with a tensile force applied to the member in the second stage of research.

crack widths. After the first stage, the tension on the rod was released to a tensile force of 1 kN. Then a load was applied with a speed of 0.01 mm/s to the value of 110 kN, until the reinforcement yielded (stresses at a level of 550 MPa; Figure 19).

Figure 20 shows the changes in fibre strain along successive measurement sections from A to F (Figure 12(b)) in the following cases: release to 1 kN and loading to 40, 70 and 100 kN. After unloading the cracked reinforced concrete member, the cracks were not completely closed as this process is limited by wedging of the aggregate and cement matrix. In addition, as a result of slipping within the contact surface between the fibre jacket and the concrete, as well as between the jacket and the internal glass core and cladding, these glass elements were moved along the member under test. This caused a specific 'freezing' of fibre strain levels. When the element was under a load of 1 kN, the crack widths measured using the Brinell magnifier glass were 0.025 mm on average.

In the next load step (up to 40 kN), further strains and increases in crack widths were observed. One of them (No. 5) was developed on the opposite surface (see Figure 20(a) and (e)). In addition, two further cracks namely Nos 7 and 8 were created, which were visible only on the more tensile and lateral surface of the member (see Figure 20(a) and (b)) for a length of about 20 mm. However, based on the results obtained by measurements (Figure 20(e)), it can be concluded that they further developed to at least half the cross section height. During the subsequent load levels, that is, 70 and 100 kN, further increases in strains and crack widths were observed.

Figure 21 shows the stress calculated on the basis of the strain on the fibre glued to the reinforcing bar. The results were inflated due to the stronger adhesion of the fibre to the concrete. For subsequent load levels, the stresses on the reinforcing steel through the crack cross section should be approximately (assuming the steel bar area as $A = 201\ \text{mm}^2$): $P/A = 5$, 199, 348 and 497 MPa, while the mean values calculated from the optical fibre strains within the crack cross section were 41, 260, 416 and 570 MPa, respectively. These results indicate the need to develop more efficient techniques for strain transfer from the steel bar to the glass core. Some attempts have been made in this area,[26] but usually spot-based or quasi-continuous measurements are involved in such an analysis. Studies showing the mechanism of transferring strains from the deformed medium into the glass core by protective coatings and jackets, including theoretical equations and laboratory investigations, are available in the literature.[18,19]

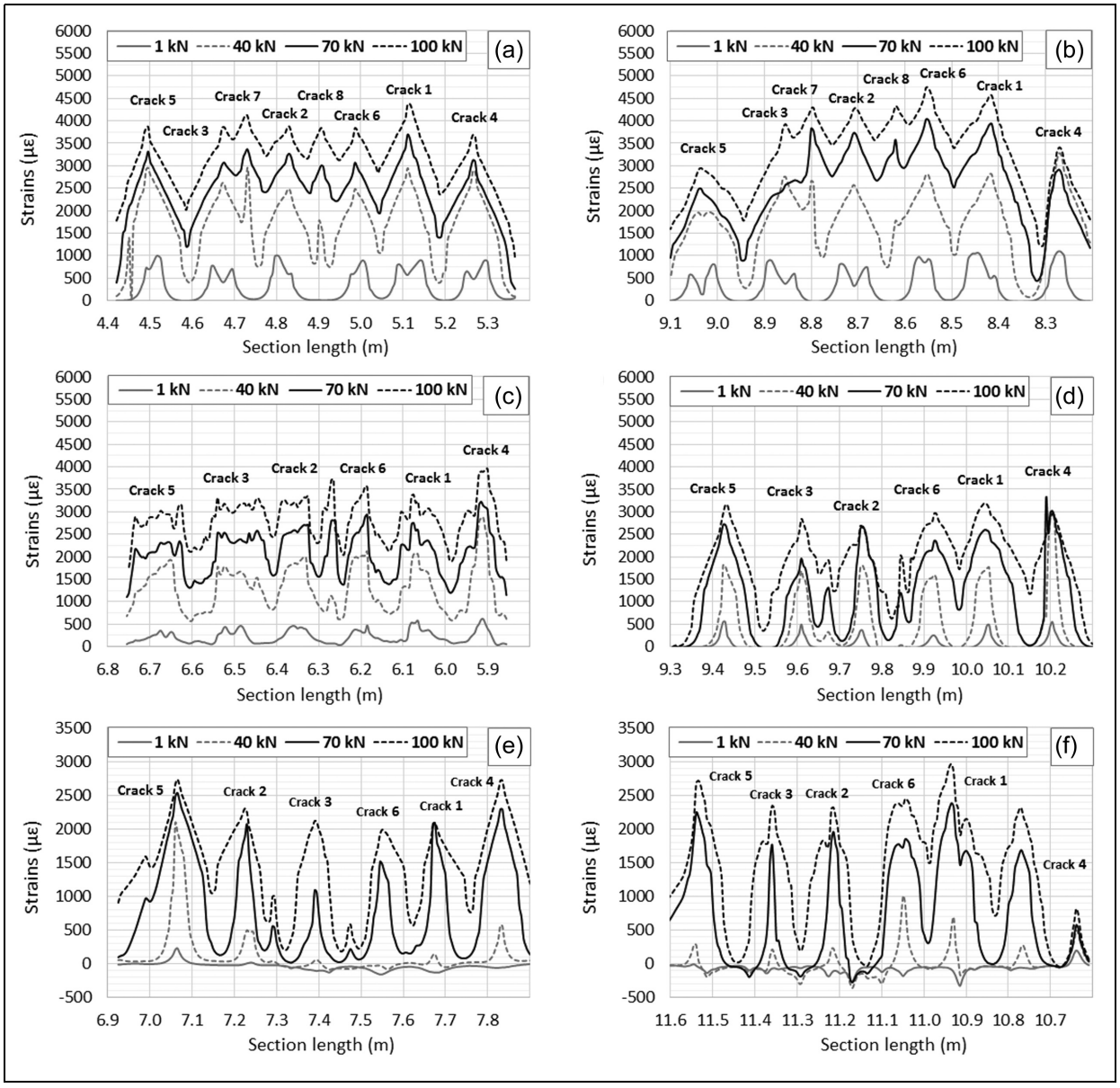

Figure 20. Changes in optical fibre strains measured during the second stage of research, on successive measurement sections (Figure 12(b)): (a) top centre, (b) top right, (c) on the reinforcing bar, (d) centre right, (e) bottom centre and (f) bottom right.

The analysis of fibre elongations within individual sections was conducted in the same way as in the first stage. Then, for the sections between the cracks (I–VI), the total elongation of the fibre was determined and equated with the upper limit of the widths of crack openings. These results, together with the measurements carried out with a Brinell magnifying glass, are summarised in Table 3.

Because of the sliding of the glass core against the plastic jacket during large deformations, and consequent summation of the fibre strains produced in the first stage of the research, the results were very high in the case of newly formed cracks (No. 7 – section IIa and No. 8 – section IIIa). In further studies, attention should be paid to the development of an effective means of strain transfer from the medium under test to the fibre glass core.

When analysing other cracks, the compatibility was definitely better. The averaged difference between measurements, overestimating and underestimating in comparison to Brinell magnifying glass measurements (Figure 22), was 0.041 and 0.018 mm, respectively. However, it should be emphasised that Brinell magnifying glass measurements were conducted on the surface

Table 3. Total fibre elongations within the sections defined in Figure 15 (I–VI) in the second stage of research (mm).

Section	Tensile force (kN)	Elongations (mm) on sections corresponding to individual cracks								Mean value (mm)	
		I	II	IIa	III	IIIa	IV	V	VI	For six cracks	For eight cracks
A	1	0.02	0.02	–	0.02	–	0.02	0.03	0.03	0.02	–
	40	0.13	0.09	0.08	0.09	0.05	0.10	0.12	0.15	0.11	0.10
	70	0.17	0.13	0.13	0.12	0.10	0.13	0.17	0.20	0.15	0.14
	100	0.21	0.17	0.17	0.15	0.14	0.17	0.22	0.26	0.20	0.19
B	1	0.02	0.02	–	0.02	–	0.02	0.03	0.02	0.02	–
	40	0.12	0.10	0.07	0.10	0.05	0.12	0.12	0.12	0.11	0.10
	70	0.14	0.12	0.12	0.16	0.11	0.20	0.21	0.11	0.16	0.15
	100	0.19	0.17	0.15	0.19	0.12	0.23	0.26	0.16	0.20	0.18
B	1	0.025	0.025	–	0.025	–	0.025	0.025	0.025	0.03	–
Brinell Magnifier glass	40	0.050	0.075	0.025	0.075	0.025	0.075	0.075	0.050	0.07	0.06
	70	0.125	0.150	0.050	0.200	0.050	0.200	0.250	0.125	0.18	0.14
	100	0.200	0.150	0.075	0.150	0.050	0.200	0.300	0.150	0.19	0.16
C	1	0.01	0.02	–	0.02	–	0.01	0.02	0.01	0.02	–
	40	0.11	0.09	0.03	0.08	0.03	0.09	0.09	0.08	0.09	0.07
	70	0.17	0.14	0.05	0.12	0.06	0.13	0.14	0.13	0.14	0.12
	100	0.24	0.18	0.07	0.16	0.08	0.18	0.19	0.18	0.19	0.16
D	1	0.00	0.00	–	0.00	–	0.00	0.00	0.00	0.00	–
	40	0.04	0.03	0.00	0.03	0.00	0.04	0.04	0.04	0.04	0.03
	70	0.11	0.05	0.02	0.07	0.01	0.10	0.12	0.09	0.09	0.07
	100	0.16	0.12	0.04	0.12	0.02	0.15	0.16	0.17	0.15	0.12
E	1	0.00	0.00	–	–0.01	–	–0.01	–0.01	0.00	0.00	–
	40	0.04	0.01	0.00	0.00	0.00	0.00	0.00	0.01	0.01	0.01
	70	0.13	0.05	0.01	0.02	0.00	0.03	0.05	0.09	0.06	0.05
	100	0.19	0.11	0.01	0.08	0.01	0.07	0.10	0.15	0.12	0.09
F	1	0.00	–0.01	–	–0.01	–	–0.01	–0.01	0.00	–0.01	–
	40	0.00	–0.01	–	–0.01	–	0.00	0.00	0.00	0.00	–
	70	0.07	0.01	–	0.03	–	0.08	0.12	0.01	0.05	–
	100	0.11	0.10	–	0.08	–	0.14	0.21	0.03	0.11	–

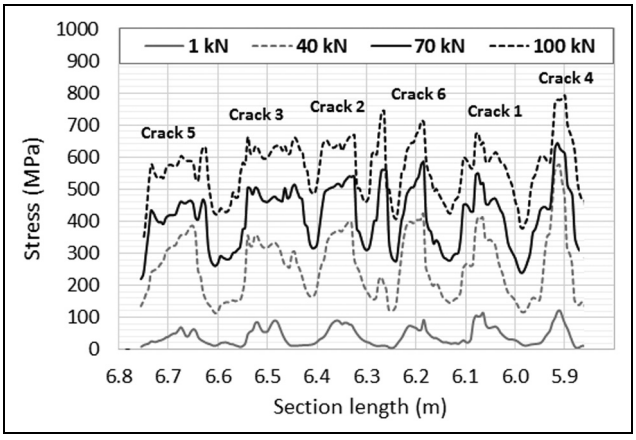

Figure 21. Changes in stress in the reinforcing bar calculated on the basis of strains measured by the glued section C of the optical fibre (second stage of research).

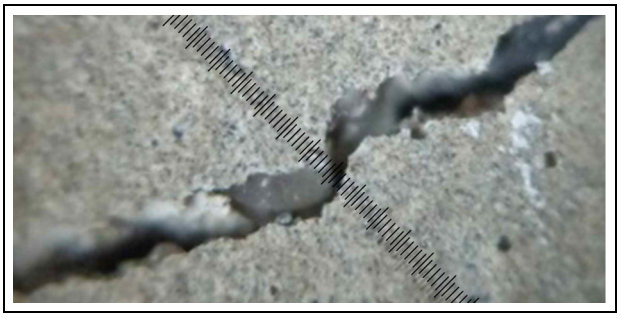

Figure 22. Crack measurement using a Brinell magnifying glass during a tensile test.

rather than inside the member and that the total accuracy depends on the position of the glass (in the reinforced concrete members, the crack width varies over the section between the reinforcing bars), due to a reading accuracy of ±0.0125 mm. By comparing the mean values of the crack widths determined on six basic cracks, the differences between the optical fibre and Brinell magnifying glass measurements were 0.01, 0.04, 0.02 and 0.01 mm for successive load steps.

In Figure 23, as shown in Table 3, total fibre elongations within the sections (from I to VI) measured between the cracks were presented. These values can be equated with the upper limit of the crack opening widths.

Conclusion

Crack analysis of concrete members is crucial in the context of the assessment of their technical condition and safety.[27] Very often, there is a need to perform monitoring and control of crack widths in reinforced concrete structures in areas where there are large levels

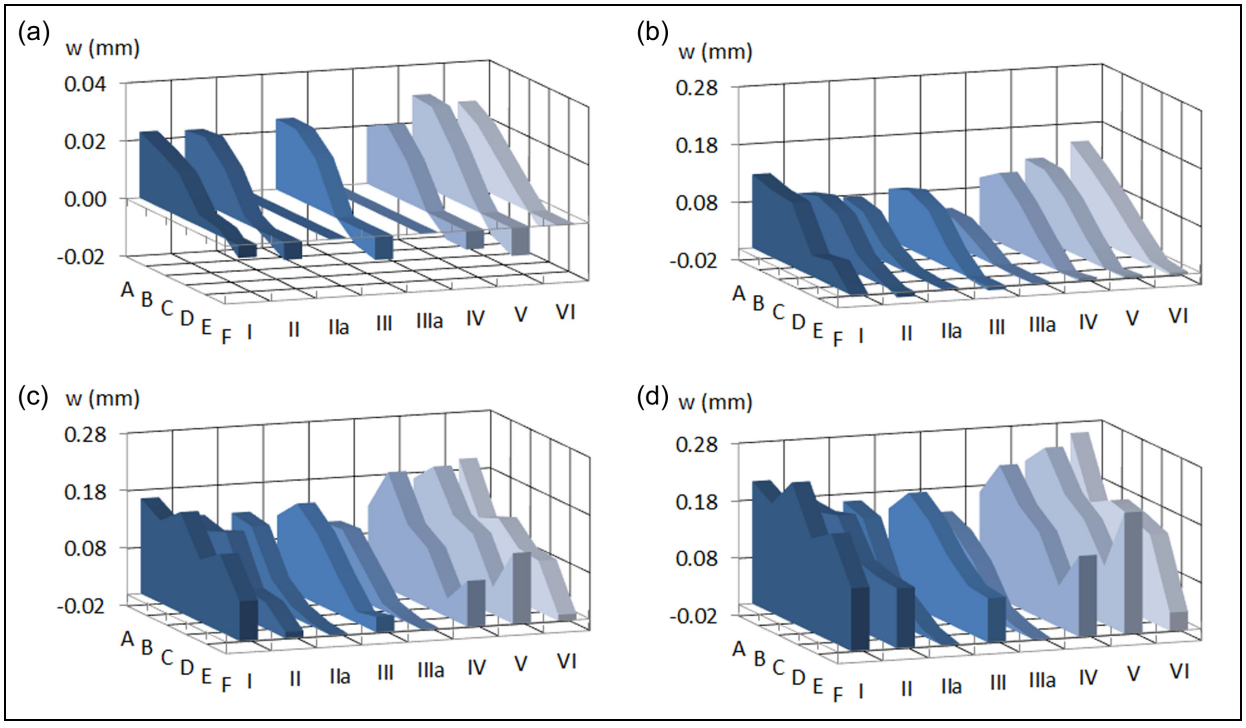

Figure 23. Total fibre elongations within sections (I–VI) measured between cracks under the following loads: (a) 1 kN, (b) 40 kN, (c) 70 kN and (d) 100 kN.

of localised strain.[28] This is the reason why work and studies are ongoing to improve the methods used in this field.[29] Based on the research carried out and presented in this article, it can be concluded that the fibre optic technology DFOS provides new opportunities in comparison with traditional spot measuring techniques (e.g. inductive, electrical resistance and vibrating wire) in the quantitative and qualitative assessment of cracks in concrete.

Measurements of strains along the entire length of the optical fibre with a spatial resolution starting from 5 mm allow the precise determination of the time and the place where these occur and/or changes in crack width. Very accurate results of measurements were obtained within the range of crack widths up to 0.05 mm. Thanks to the application of DFOS, it was possible to analyse microcracks invisible to the naked eye.

In the case of the crack widths of 0.1–0.3 mm, the difference was greater in comparison with the reference measurements made with the Brinell magnifying glass. This phenomenon was mainly due to the presence of a tight plastic jacket protecting the glass core of the fibre. This jacket allowed the core (measuring element) to slip between the more and less tensioned zones. Therefore, the fibre strains did not correspond fully with the actual deformation state of the concrete member. However, the method of measurement described allowed for very precise determination of the crack widths as the sum of fibre elongations (strains integral) within the sections between the cracks. Thus, despite using optical fibres in a tight jacket which mediates in strain transfer, the results obtained could be very suitable for the assessment of the structural condition of the members under consideration.

It is also worth underlining that the tests conducted indicate the effectiveness of distributed optical fibre technology not only for strain measurement within a tensile area (discontinuities resulting from the occurrence of cracks), but also in the analysis of concrete homogeneity and its structural behaviour within compressed areas, as it is possible to calculate strains over very short measurement bases – see Figures 7 and 10.

The research and the results presented in this article confirm the great technical possibilities of strain measurements within cracked concrete structural members with DFOS technology, which allow for a very accurate analysis of strain distributions and cracks occurring along the measuring line. Attention should also be paid to the limitations of optical fibre measurement technology, which are connected mainly with the following issues:

- Possibility of breaking the measuring fibre during the installation process;
- Difficulties in stabilising the slender measurement fibre inside the concrete structural member in the design position;
- Difficulties in adopting the model of strain transfer from the medium under test through protective coatings on the glass fibre (the necessity of taking into account many parameters such as adhesion between concrete and protective coating, adhesion between the protective coating and the glass core, parameters of adhesive agent used for the fibre installation on the concrete surface or reinforcing bar);
- High price of the optical reflectometer and its software;
- The possibility of breaking the optical fibre with wide cracks (the limit strains declared by producers at the level of 3% may not be sufficient due to the locality of the crack phenomenon).

The studies presented show both the advantages and disadvantages of applied measurement techniques, which require improvement, primarily within the field of strain transfer from the medium under test, through the protective layers of the fibre, to its glass core and cladding.

Declaration of conflicting interests

The author(s) declared no potential conflicts of interest with respect to the research, authorship and/or publication of this article.

Funding

The author(s) received no financial support for the research, authorship and/or publication of this article.

ORCID iD

Tomasz Howiacki https://orcid.org/0000-0002-6833-7203

References

1. Bednarski Ł and Sieńko R. Pomiary odkształceń konstrukcji czujnikami strunowymi [Strain measurements with vibrating wire sensors]. *Inżynieria I Budownictwo* 2013; 11: 615–619.
2. López-Higuera JM, Rodriguez L, Quintela A, et al. Currents and trends on fiber sensing technologies for structural health monitoring. In: *Proceedings of the 2nd Mediterranean photonics conference*, Eilat, Israel, 29 November–2 December 2010.
3. Samiec D. Distributed fibre-optic temperature and strain measurement with extremely high spatial resolution. *Photonik International*, 2012, http://lunainc.com/wp-content/uploads/2013/04/photonik_intl_2012_010.pdf
4. Delepine-Lesoille S, Merliot E, Boulay C, et al. Quasi-distributed optical fibre extensometers for continuous

embedding into concrete: design and realization. *Smart Materials and Structures* 2006; 15: 931–938.
5. Zhou Z, Wang B and Ou J. Local damage detection of RC structures with distributive FRP-OFBG sensors. In: *Proceedings of the second international workshop on structural health monitoring of innovative civil engineering structures*, Winnipeg, MB, Canada, 23–24 September 2004.
6. Li W and Bao X. High spatial resolution distributed fiber optic technique for strain and temperature measurements in concrete structures. In: *Proceedings of the international workshop on smart materials & structures, SHM and NDT for the energy industry*, Calgary, AB, Canada, 7–10 October 2013.
7. Bernini R, Minardo A, Ciaramella S, et al. Distributed strain measurement along a concrete beam via stimulated Brillouin scattering in optical fibers. *Int J Geophys* 2011; 2011: 710941.
8. Froggatt M, Gifford D, Kreger S, et al. Distributed strain and temperature discrimination in unaltered polarization maintaining fiber. *Luna Technologies*, 2012, https://lunainc.com/wp-content/uploads/2012/08/Strain-and-Temperature-in-PM-Fiber.pdf
9. Culshaw B and Kersey A. Fibre-optic sensing: a historical perspective. *J Lightwave Technol* 2008; 26(9): 1064–1078.
10. López-Higuera JM, Rodriguez L, Quintela A, et al. Fiber optic sensors in structural health monitoring. *J Lightwave Technol* 2011; 29(4): 587–608.
11. Minardo A, Bernini R, Amato L, et al. Bridge monitoring using Brillouin fiber-optic sensors. *IEEE Sens J* 2012; 12(1): 145–150.
12. Minardo A, Persichetti G, Testa G, et al. Long term structural health monitoring by Brillouin fiber-optic sensing: a real case. *J Geophys Eng* 2012; 9(2012): S64–S69.
13. Barrias A. Concrete structures monitoring with OBR based distributed optical fiber sensors (DOFS). In: *Proceedings of the COST TU1402: quantifying the value of structural health monitoring*, Copenhagen, 24 August 2016.
14. Barrias A, Casas JR and Villalba S. A review of distributed optical fiber sensors for civil engineering applications. *Sensors* 2016; 16: 748.
15. Barrias A, Casas JR and Herrero SV. Review of civil engineering applications with distributed optical fiber sensors. In: *Proceedings of the 8th European workshop on structural health monitoring (EWSHM 2016)*, Bilbao, 5–8 July 2016.
16. Glišić B and Inaudi D. *Fibre optic methods for structural health monitoring*. Hoboken, NJ: John Wiley & Sons, 2007.
17. Measures RM. *Structural monitoring with fiber optic technology*. Cambridge, MA: Academic Press, 2001.
18. Li D, Ren L and Li H. Mechanical property and strain transferring mechanism in optical fiber sensors. In: Yasin M, Harun SW and Arof H (eds) *Fiber optic sensors*. New York: InTech, 2012, pp. 439–458.
19. Billon A, Henault JM, Quiertant M, et al. Quantitative strain measurement with distributed fiber optic systems: qualification of a sensing cable bonded to the surface of a concrete structure. In: *Proceedings of the 7th European workshop on structural health monitoring*, Nantes, 8–11 July 2014.
20. Evano N, Abdi RE and Poulain M. Lifetime modeling of silica optical fiber in static fatigue test. *J Appl Res Technol* 2016; 14: 278–285.
21. Feng X, Zhou J, Sun C, et al. Theoretical and experimental investigations into crack detection with BOTDR-distributed fiber optic sensors. *J Eng Mech* 2013; 139(12): 622.
22. Imai M and Feng M. Sensing optical fibre installation study for crack identification using stimulated Brillouin-based strain sensor. *Struct Health Monit* 2012; 11(5): 501–509.
23. Güemes A, Fernández-López A and Soller B. Optical fiber distributed sensing – physical principles and applications. *Struct Health Monit* 2010; 9(3): 233–245.
24. Gifford D, Soller B, Wolfe M, et al. Distributed fiber-optic sensing using Rayleigh backscatter. In: *European conference on optical communications (ECOC) technical digest*, Glasgow, 25–29 September 2005.
25. Luna Innovations Inc. *User guide, optical backscatter reflectometer 4600*. Roanoke, VI: Luna Innovations Inc., 2013.
26. Sahay P, Kaya M and Wang CH. Fiber loop ringdown sensor for potential real-time monitoring of cracks in concrete structures: an exploratory study. *Sensors* 2013; 13: 39–57.
27. Seruga A and Zych M. Thermal cracking of the cylindrical tank under construction. I: case study. *Am Soc Civil Eng ASCE: J Perform* 2015; 29(4): 581.
28. Zych M. Research on thermal cracking of a rectangular RC tank wall under construction. II: comparison with numerical model. *Am Soc Civil Eng ASCE: J Perform* 2016; 30(1): 703.
29. Sieńko R, Howiacki T, Szydłowski R, et al. Application of distributed optical fiber sensor technology for strain measurements in concrete structures. In: *Proceedings of the COST TU1402, quantifying the value of structural health monitoring*, Copenhagen, 24 August 2016.